Techset Composition Ltd, Salisbury
Doc: {IEE}CDs/Articles/Pagination/CDS57344.3d

Published in IET Circuits, Devices & Systems
Received on 9th March 2009
Revised on 8th May 2009
doi: 10.1049/iet-cds.2009.0062

ISSN 1751-858X

On the two-port network classification of Colpitts oscillators

A.S. Elwakil

Q1 *Department of Electronic and Computer Engineering, University of Sharjah, P.O. Box 27272, United Arab Emirates*
E-mail: elwakil@ee.ucd.ie

Abstract: Using two-port network representations, we classify Colpitts oscillators into three categories based on the specific active device terminal which is grounded. General and accurate characteristic equations which are independent of any particular transistor (or active device) model are derived for all three classes. Possible two-impedance two-port network oscillators are also analysed.

1 Introduction

Two-port network analysis techniques form a basic part of elementary textbooks in circuit theory [1] and are relatively old and well-established techniques [2]. On the other hand, the Colpitts oscillator (shown in Fig. 1*a*) is a classical and widely used oscillator circuit particularly in high-frequency communication systems [3–5]. However, several variants of this oscillator appear in the literature and are
Q2 also referred to as Colpitts oscillators such as the MOS transistor-based circuit of Fig. 1*b* and the BJT one of Fig. 1*e*. A common feature among these circuits is that the oscillation frequency is ideally expressed as $\omega_o = 1/\sqrt{LC_{\text{eff}}}$, where $C_{\text{eff}} = C_1C_2(C_1 + C_2)$, hence allowing the capacitive divider to effectively tune the frequency. However, three questions need to be answered; in particular:

1. Are the various Colpitts oscillators of Fig. 1 structurally equivalent?

2. Can all these structures be implemented using bipolar or MOS transistors?

3. Is the common assumption that the Colpitts oscillator is effectively a second-order system if the employed transistor is modelled as a linear device (i.e. under small-signal conditions) valid for all structures? Of course, it is well known that oscillators are strong non-linear circuits and accurate modelling of the Colpitts oscillator implies that it is a third-order non-linear system [6–9]. However, the first step in the analysis or design of an oscillator is usually to consider a linearised (with respect to the equilibrium point at the origin) model from which an *s*-domain characteristic equation is derived and the oscillation start-up condition (Hopf bifurcation condition) and oscillation frequency can then be estimated [10]. This follows the classical Barkhausen oscillation criteria which is a necessary but insufficient condition [11].

In this work, we show based on two-port network modelling that:

1. Three generic structures of Colpitts oscillators, named common-A, common-B and common-C, can exist. The characteristic equation of each class is distinct and not similar to any of the others. We derive the characteristic equations as functions of the two-port network transmission parameters defined as

$$\begin{pmatrix} V_1 \\ I_1 \end{pmatrix} = \begin{pmatrix} a_{11} & a_{12} \\ a_{21} & a_{22} \end{pmatrix} \begin{pmatrix} V_2 \\ -I_2 \end{pmatrix} \tag{1}$$

where V_1 and I_1 are the input port voltage and current whereas V_2 and I_2 are the output port voltage and current, respectively (see Fig. 2*a*).

2. The common-A structure is a degenerate second-order system which can be implemented both by using the BJT and MOS transistors. However, the common-B structure remains a third-order oscillator and does not degenerate into a second-order system with linear small-signal

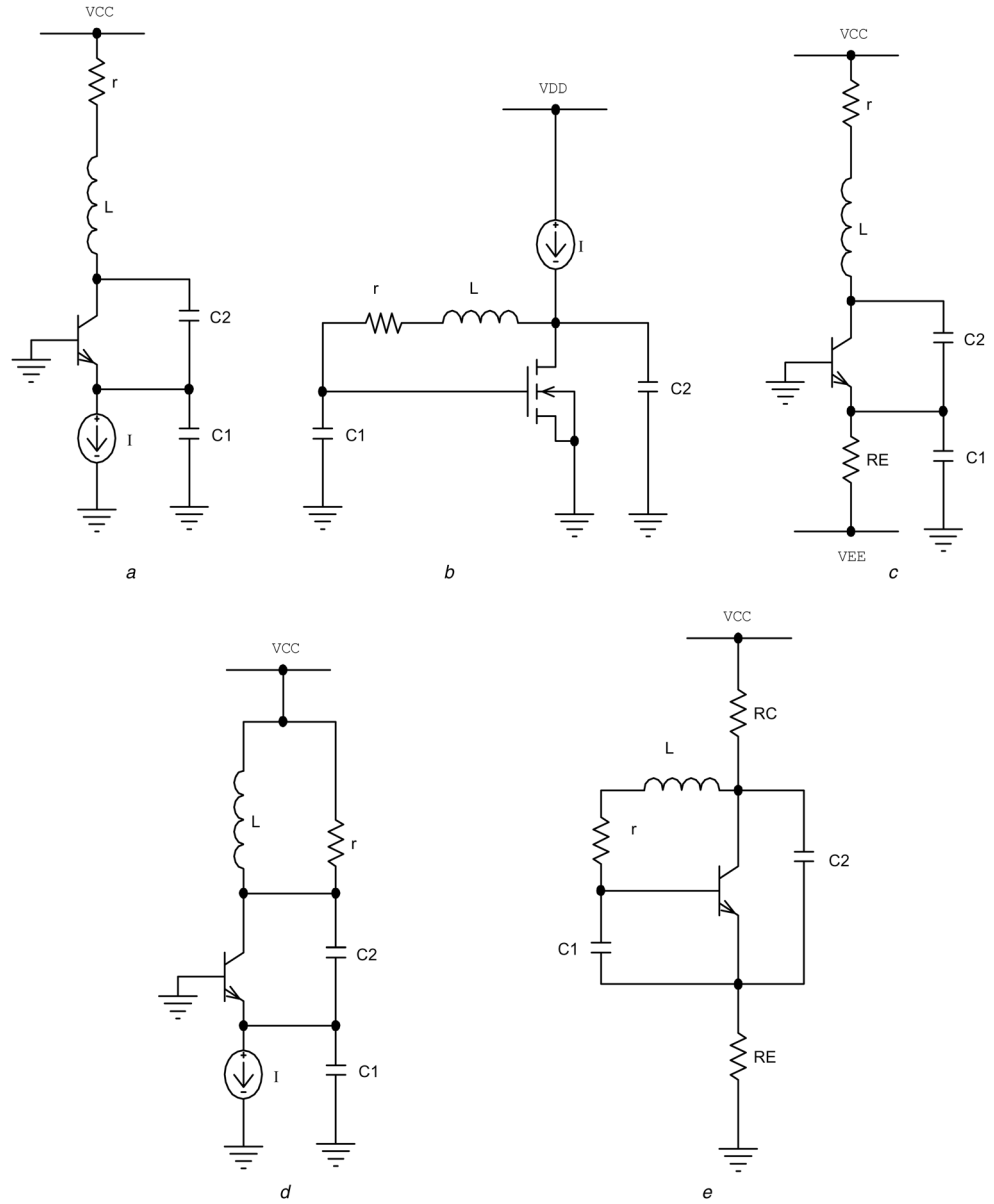

Q3 **Figure 1** *Examples of classical Colpitts oscillators using BJT and MOS transistors*

transistor models. This structure can also be implemented both by using BJT and MOS transistors.

In order to proceed forward, it is important to derive here the transmission parameters for the small-signal equivalent circuits of BJT and MOS transistors. The use of the transmission matrix is particularly suited for networks with feedback [12].

2 BJT and MOS transistor transmission parameters

Q2 Fig. 2*b* shows the small-signal equivalent circuit of an NPN BJT transistor operating in the forward active mode. The model comprises two terminal resistors (r_b, r_e) (ideally $r_e = 0$) and a dependent current-controlled current source βI_1 with output resistance r_o. β is the forward active current gain (assumed constant) and r_b is related to the BJT small-signal transconductance g_m as $r_b = \beta/g_m$. It can be shown that the (*a*) matrix for this equivalent circuit is

$$\begin{pmatrix} a_{11} & a_{12} \\ a_{21} & a_{22} \end{pmatrix} = \frac{-1}{\beta r_o - r_e} \begin{pmatrix} r_b + r_e & \beta r_e r_o + r_b(r_o + r_e) \\ 1 & r_o + r_e \end{pmatrix} \tag{2}$$

The above (*a*) may be simplified considering that $\beta r_o \gg r_e$ and $(1/\beta r_o) \to 0$ and then becomes

$$\begin{pmatrix} a_{11} & a_{12} \\ a_{21} & a_{22} \end{pmatrix} = \begin{pmatrix} \dfrac{-1}{g_m r_o} & -\left(r_e + \dfrac{1}{g_m} + \dfrac{r_e}{g_m r_o}\right) \\ 0 & \dfrac{-1}{\beta} \end{pmatrix}$$

doi: 10.1049/iet-cds.2009.0062

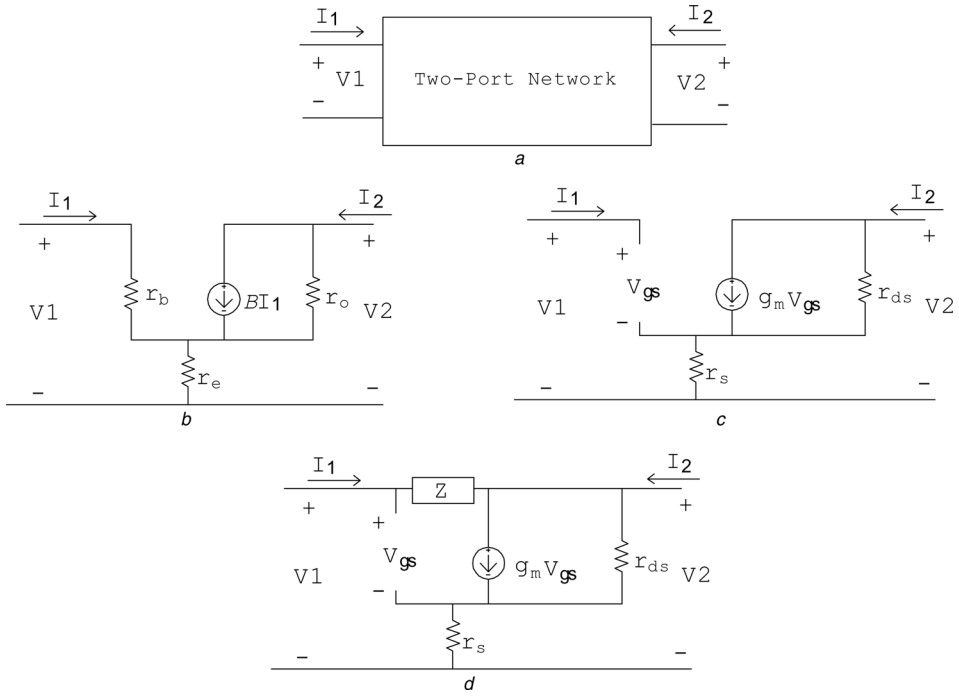

Q4 Figure 2

a Two-port network variables
b Basic small signal equivalent model of a BJT transistor
c Basic small signal equivalent model of a MOS transistor
d MOS transistor model with a gate-to-drain impedance *Z*

$$= \begin{pmatrix} \dfrac{-1}{A} & -\left[r_e\left(1+\dfrac{1}{A}\right)+\dfrac{1}{g_m}\right] \\ 0 & \dfrac{-1}{\beta} \end{pmatrix} \tag{3}$$

where $A = g_m r_o$. If A is sufficiently large such that $(1/A) \rightarrow 0$, a further simplification yields

$$\begin{pmatrix} a_{11} & a_{12} \\ a_{21} & a_{22} \end{pmatrix} = \begin{pmatrix} 0 & -\left(r_e+\dfrac{1}{g_m}\right) \\ 0 & \dfrac{-1}{\beta} \end{pmatrix} \tag{4}$$

In a similar manner, and recalling the small-signal equivalent circuit of a MOS transistor operating in the saturation mode (Fig. 2*c*), it can be shown that the (*a*) matrix for this circuit is

$$\begin{pmatrix} a_{11} & a_{12} \\ a_{21} & a_{22} \end{pmatrix} = \frac{-1}{g_m r_{ds}} \begin{pmatrix} 1 & r_s(1+g_m r_{ds})+r_{ds} \\ 0 & 0 \end{pmatrix} \simeq \begin{pmatrix} \dfrac{-1}{g_m r_{ds}} & -\left(r_s+\dfrac{1}{g_m}\right) \\ 0 & 0 \end{pmatrix} \tag{5}$$

where g_m is the small-signal transconductance, r_{ds} is the drain to source resistance and r_s is the source resistance (ideally $r_s = 0$). It is worth noting that under the ideal conditions $(r_e, r_o, \beta) = (0, \infty, \infty)$ for the BJT and $(r_s, r_{ds}) = (0, \infty)$ for the MOS, both transistors can be described by the ideal transmission matrix

$$\begin{pmatrix} a_{11} & a_{12} \\ a_{21} & a_{22} \end{pmatrix} = \begin{pmatrix} 0 & -1/g_m \\ 0 & 0 \end{pmatrix} \tag{6}$$

where the transconductance g_m is the only design parameter.

3 Three-impedance two-port structures

Here we consider a generic two-port network terminated at its input by an impedance Z_1, at its output by an impedance Z_2 whereas a feedback impedance Z_3 is connected from output to input. One such structure is shown in Fig. 3*a*. Note that this structure has three nodes marked as *A*, *B* and *C* with node *A* common ground. Two more structures are shown, respectively, in Figs. 3*b* and *c* where alternatively nodes *B* and *C* are common ground.

3.1 Common-A structure

Recalling this structure, shown in Fig. 3*a*, it is clear that $I_{Z1} = -I_{Z2}$ and hence $V_1/V_2 = -Z_1/Z_2$. Also, $I_2 = I_{Z3} - I_{Z2} = V_1/Z_3 - [(1/Z_2) + (1/Z_3)]V_2$. Using both expressions and the matrix (1) yields $V_1/V_2 = [a_{11} + (a_{12}/Z_2) + (a_{12}/Z_3)]/[1 + (a_{12}/Z_3)]$. Hence, the general

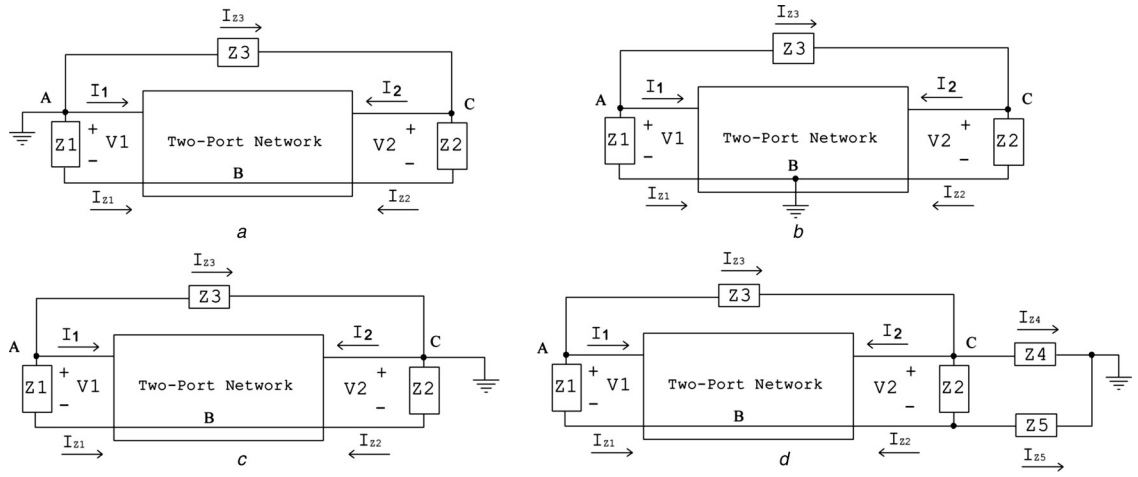

Figure 3 *Possible three-impedance two-port network connections*

a Common-A topology
b Common-B topology
c Common-C topology
d Modified common-C topology

characteristic equation of this structure is

$$\frac{-Z_1}{Z_2} = \frac{a_{11} + a_{12}((1/Z_2) + (1/Z_3))}{1 + (a_{12}/Z_3)} \tag{7}$$

To obtain a Colpitts oscillator, the impedance settings are $Z_1 = 1/sC_1$, $Z_2 = 1/sC_2$ and $Z_3 = sL + r$. Recalling (4) and substituting in (7), we derive the characteristic equation of this common-A Colpitts oscillator if implemented using a BJT as

$$s^2 + \frac{(r_e + (1/g_m))C_1 r - L}{(r_e + (1/g_m))C_1 L} s + \left(\frac{C_1 + C_2}{C_1 C_2 L} - \frac{r}{(r_e + (1/g_m))C_1 L}\right) = 0 \tag{8}$$

which has pure imaginary roots (oscillation start-up condition) if

$$\frac{L/C_1}{r} = r_e + \frac{1}{g_m} = \frac{1}{g_m}|_{r_e \to 0} \tag{9}$$

and the oscillation frequency in this case is

$$\omega_o = \sqrt{\frac{1}{LC_{eff}} - \left(\frac{r}{L}\right)^2} = \frac{1}{\sqrt{LC_{eff}}}|_{r \to 0} \tag{10}$$

where $C_{eff} = C_1 C_2/(C_1 + C_2)$. Practically and in order to ensure start-up, the poles need to be slightly shifted into the right-half plane by increasing g_m [$g_m > r/(L/C_1)$]. The Colpitts oscillator circuit of Fig. 1*a* belongs to this class. Note from (10) that there is a limitation on the maximum value of C_{eff} ($C_{eff} < L/r^2$) in order to ensure a positive value of ω_o.

Now recalling (5) and substituting again in (7) we obtain the characteristic equation of a common-A Colpitts oscillator implemented using a MOS transistor as

$$s^2 + \frac{(r_s + (1/g_m))C_1 r + (LC_1/g_m r_{ds} C_2) - L}{(r_s + (1/g_m))C_1 L} s + \left(\frac{C_1 + C_2}{C_1 C_2 L} + \frac{C_1 r/g_m r_{ds} - C_2 r}{(r_s + (1/g_m))C_1 C_2 L}\right) = 0 \tag{11}$$

which yields the oscillation start-up condition as

$$\frac{L/C_1}{r} = r_s + \frac{1}{g_m} + \frac{L/C_2}{r g_m r_{ds}} = \frac{1}{g_m}|_{r_{ds} \to \infty, r_s \to 0} \tag{12}$$

and the oscillation frequency in this case is the same as that given by (10).

It is thus clear that the common-A structure can be implemented both by using BJT and MOS transistors. It is particularly noted that for both BJT and MOS implementations, the characteristic equation (7) simplifies uniquely to

$$Z_1 + Z_2 + Z_3 - g_m Z_1 Z_3 = 0 \tag{13}$$

under the conditions $r_e = r_s = 0$ and $r_{ds} = \infty$.

The Colpitts oscillator in Fig. 1*c* also belongs to this class. Compared to Fig. 1*a*, note that the current source is replaced with resistance R_E. Repeating the analysis above after considering that Z_1 in this case equals $(R_E + 1/sC_1)$, it can be shown that the oscillation start-up condition and

doi: 10.1049/iet-cds.2009.0062

oscillation frequency become

$$\frac{rR_E + L/C_1}{r + R_E} = r_e + \frac{1}{g_m} \Rightarrow \frac{L/C_1}{R_E} = \frac{1}{g_m}|_{r\to 0, r_e \to 0} \quad (14a)$$

and

$$\omega_o = \sqrt{\frac{L + rR_EC_1}{LC_{eff}(L - R_E^2C_1)} - \frac{r^2}{L^2 - R_E^2C_1L}} = \frac{1}{\sqrt{C_{eff}(L - R_E^2C_1)}}|_{r\to 0} \quad (14b)$$

with the constraint on the maximum value of C_{eff} ($C_{eff} < (L/r^2) + (R_EC_1/r)$). Note that in the above analysis we used the simplified matrices of (4) and (5). We may use more sophisticated matrices, such as (2) if we seek higher accuracy.

Other examples of Colpitts oscillators belonging to this topology can be seen in [13–15] using a MOS transistor and in [16] using a BJT. These examples when compared to Fig. 1*a* are different only in that the inductor L is placed in parallel (instead of in series) with the resistance r, as shown in Fig. 1*d*. Using (13) with $Z_3 = sL/(r + sL)$ in this case one obtains the characteristic equation

$$s^2 + \left(\frac{C_1 + C_2}{C_1C_2r} - \frac{g_m}{C_1}\right)s + \frac{C_1 + C_2}{C_1C_2L} = 0 \quad (15)$$

which leads to the start-up condition $(1/g_m) = r/[1 + (C_1/C_2)]$ and oscillation frequency $\omega_o = 1/\sqrt{LC_{eff}}$.

3.2 Common-B structure

Recalling Fig. 3*b* of this structure it can be seen that $I_1 = -(I_{Z1} + I_{Z3}) = V_1/Z_3 - [(1/Z_1) + (1/Z_3)]V_2$. Also $I_2 = I_{Z3} - I_{Z2} = V_1/Z_3 - [(1/Z_2) + (1/Z_3)]V_2$. Substituting these expressions into the matrix equations (1) yields the characteristic equation of this structure as

$$\frac{Z_1(a_{12} + Z_3)}{Z_1(1 - a_{22}) + Z_3} = \frac{a_{12}(Z_2 + Z_3) + a_{11}Z_2Z_3}{Z_2(1 - a_{22}) - a_{21}Z_2Z_3 - a_{22}Z_3} \quad (16)$$

which unlike (7) depends on all four elements of the (a) matrix. Using (4) and (5) in (16) under the conditions $r_e = r_s = 0$, $r_{ds} \to \infty$ and $\beta \to \infty$, (16) uniquely simplifies to

$$Z_1 + Z_2 + Z_3 + g_mZ_1Z_2 = 0 \quad (17)$$

for both BJT and MOS transistor implementations.

With the Colpitts impedance setting $Z_1 = 1/sC_1$, $Z_2 = 1/sC_2$ and $Z_3 = sL + r$, (17) becomes

$$s^3 + \frac{r}{L}s^2 + \frac{C_1 + C_2}{LC_1C_2}s + \frac{g_m}{LC_1C_2} = 0 \quad (18)$$

for which the start-up condition is

$$\frac{L/(C_1 + C_2)}{r} = \frac{1}{g_m} \quad (19)$$

and the oscillation frequency is $\omega_o = 1/\sqrt{LC_{eff}}$. Comparing (19) (which is the widely known start-up condition for the Colpitts oscillator) with (12) or (14a), it is seen that while (19) depends on both C_1 and C_2, (12) and (14a) depend only on C_1. This highlights the need for the proper classification of Colpitts oscillator topologies.

In conclusion, it is seen that the common-B structure can be realised interchangeably with BJT and MOS transistors and yields a unique third-order characteristic equation (i.e. does not degenerate into a second-order system).

3.3 Common-C structure

Fig. 3*c* represents this structure. However, a more widely used structure, which includes two extra impedances (Z_4 and Z_5) is shown in Fig. 3*d* and denoted the 'modified common-C' topology. Examples of this structure can be seen in Fig. 1 of [17] and Fig. 2 of [18]. The general characteristic equation of this topology is derived as

$$\frac{a_{11}/a_{12} + 1/Z_2 + 1/Z_3 + 1/Z_4 + Z_5/Z_2Z_4}{1/a_{12} + 1/Z_3 - Z_5/Z_1Z_4} = \frac{a_{11}a_{22}/a_{12} - a_{21} + 1/Z_3}{a_{22}/a_{12} + 1/Z_1 + 1/Z_3} \quad (20)$$

Using (4) for a BJT and assuming $r_e = 0$ and $\beta \to \infty$, (20) simplifies to

$$Z_1 + Z_3 + g_mZ_1Z_4 + \frac{(Z_1 + Z_2 + Z_3)(Z_4 + Z_5)}{Z_2} = 0 \quad (21)$$

which for $Z_1 = 1/sC_1$, $Z_2 = 1/sC_2$, $Z_3 = sL + r$, $Z_4 = R_C$ and $Z_5 = R_E$ (see e.g. Fig. 1*e*) yields

$$s^3 + \left[\frac{1}{(R_E + R_C)C_2} + \frac{r}{L}\right]s^2 + \left[\frac{r}{L(R_E + R_C)C_2} + \frac{1}{LC_{eff}}\right]s + \frac{1 + g_mR_C}{LC_1(R_E + R_C)C_2} = 0 \quad (22)$$

and hence the start-up condition and oscillation frequency are respectively

$$g_mR_C = \frac{C_1}{C_2}\left(1 + \frac{r}{R_C + R_E}\right) + \frac{r}{L}[rC_1 + (R_C + R_E)(C_1 + C_2)] = \frac{C_1}{C_2}|_{r\to 0} \quad (23a)$$

$$\omega_o = \sqrt{\frac{1}{LC_{\text{eff}}} + \frac{r}{L(R_E + R_C)C_2}} \quad = \frac{1}{\sqrt{LC_{\text{eff}}}}|_{r\to 0} \quad (23b)$$

We have simulated this circuit using a commercial Q2N2222 BJT with an ideal inductor $L = 10\ \mu H$ $(r = 0)$, $C_1 = C_2 = 1$ nF, $R_C = 1$ kΩ, $R_E = 9$ kΩ and $V_{CC} = 1.5$ V. According to Table 2, oscillations should start at a gain $g_m R_C = 1$ and render an ideal oscillation frequency of 2.25 MHz. Spice simulations results are shown in Figs. 4*a* and *b* where with the above components oscillations start at a gain of 1.12 and the oscillation frequency is measured as 2.16 MHz. Of course increasing the gain increases the amplitude of the generated waveform, as shown in Fig. 4*c* with $R_E = 2$ kΩ (gain =5) but also increases the distortion.

For a MOS transistor and using (5) in (20) assuming $r_s = 0$ and $r_{ds} \to \infty$, (20) yields the same characteristic equation (21). We have also simulated the circuit in Fig. 1*e* with a BS170 MOS transistor (with $V_{CC} = 2.5$ V) and obtained similar results. Note that the characteristic equation of Fig. 3*c* can be obtained from that of Fig. 3*d* setting $Z_4 = 0$ and $Z_5 = \infty$.

A summary of all Colpitts oscillator structures is given in Table 1 whereas a comparison of the circuits in Fig. 1 is given in Table 2.

4 Parasitic analysis using two-port networks

One of the main advantages of the derived two-port characteristic equations is that the level of accuracy in the analysis is related to the complexity of the transistor model, which reflects directly in the (*a*) matrix parameters. As such, re-analysing any of the three structures to consider the effect of a parasitic element is not needed. Instead, direct substitution in the derived expressions of Table 1 is sufficient. Consider for example the MOS transistor small-signal model of Fig. 2*d* where an impedance Z (typically a parasitic C_{gd} capacitor) is connected from gate to drain.

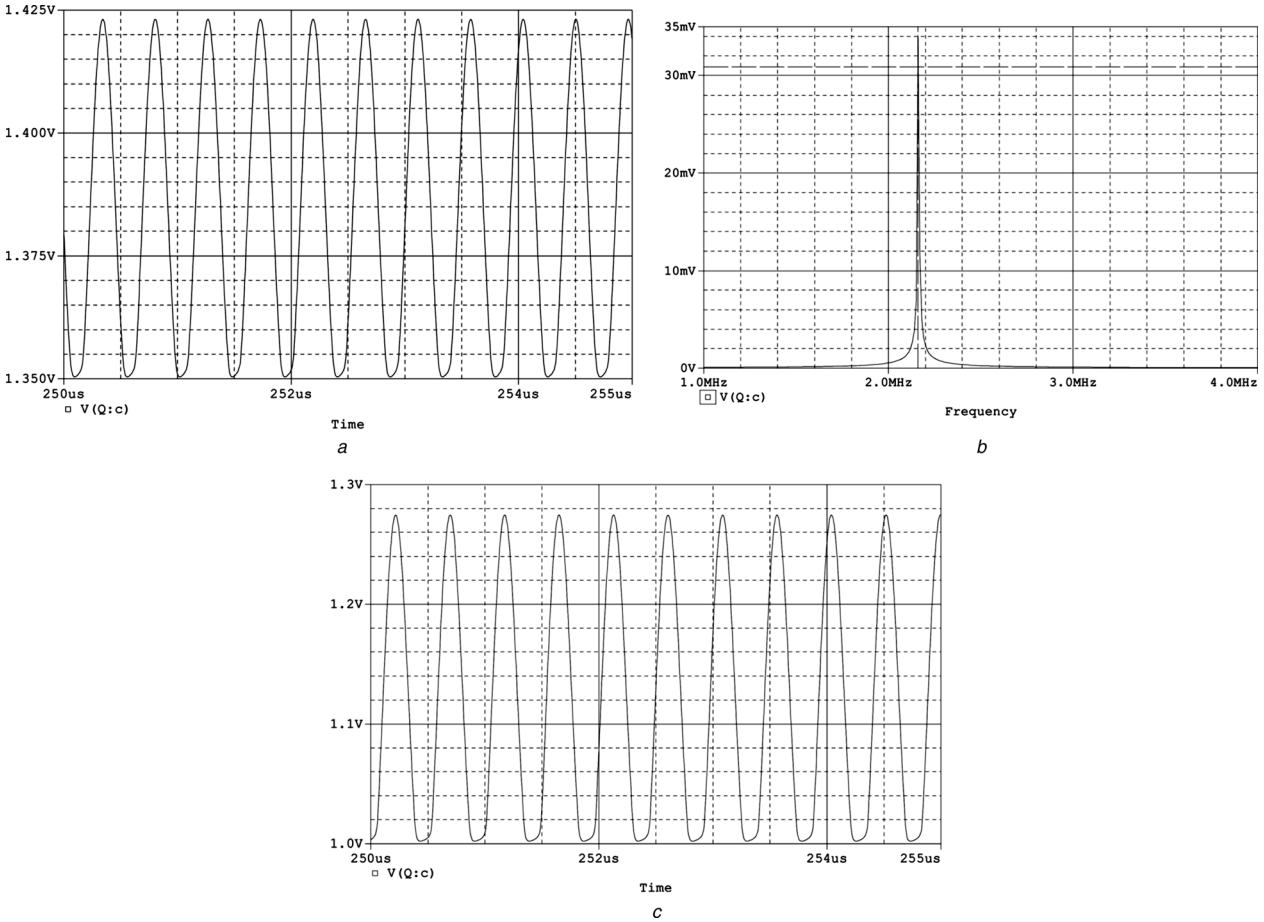

Figure 4 *Spice simulations of Fig. 1e*

a Waveform at start-up gain 1.2
b Corresponding spectrum
c Waveform at gain 5

doi: 10.1049/iet-cds.2009.0062

Table 1 Summary of characteristic equations for the structures in Fig. 3

Topology	General equation	Using BJT	Using MOS
common-A (Fig. 3*a*)] (Figs. 1*a*, *c*, *d*)	$\frac{-Z_1}{Z_2}=\frac{a_{11}+a_{12}(1/Z_2+1/Z_3)}{1+a_{12}/Z_3}$	$\frac{Z_1}{Z_2}=\frac{(1+g_m r_e)(Z_2+Z_3)}{Z_2(g_m Z_3-g_m r_e-1)}$ $\rightarrow Z_1+Z_2+Z_3-g_m Z_1 Z_3=0\vert_{r_e=0}$	$Z_1=-\frac{Z_2Z_3/r_{ds}+(1+g_m r_s)(Z_2+Z_3)}{1+g_m r_s-g_m Z_3}$ $\rightarrow Z_1+Z_2+Z_3-g_m Z_1 Z_3=0\vert_{\substack{r_s=0\\ r_{ds}=\infty}}$
common-B (Fig. 3*b*) (Fig. 1*b*)	$\frac{a_{12}+Z_3}{a_{22}-1-Z_3/Z_1}$ $=\frac{a_{12}(1/Z_2+1/Z_3)+a_{11}}{(a_{22}-1)/Z_3+a_{22}/Z_2+a_{21}}$	$\frac{Z_1(r_e+1/g_m-Z_3)}{Z_1(1+1/\beta)+Z_3}$ $=\frac{(r_e+1/g_m)(Z_2+Z_3)}{Z_2(1+1/\beta)+Z_3/\beta}$ $Z_1+Z_2+Z_3+g_m Z_1 Z_2=0\vert_{\substack{r_e=0\\ \beta=\infty}}$	$\frac{Z_1(r_s+1/g_m-Z_3)}{Z_1+Z_3}$ $=\frac{(r_s+1/g_m)(Z_2+Z_3)+Z_2Z_3/g_m r_{ds}}{Z_2}$ $\rightarrow Z_1+Z_2+Z_3+g_m Z_1 Z_2=0\vert_{\substack{r_s=0\\ r_{ds}=\infty}}$
modified common-C (Fig. 3*d*) (Fig. 1*e*)	$\frac{a_{11}/a_{12}+1/Z_2+1/Z_3}{+1/Z_4+Z_5/Z_2Z_4}$ $\frac{1/a_{12}+1/Z_3-Z_5/Z_1Z_4}{=\frac{a_{11}a_{22}/a_{12}-a_{21}+1/Z_3}{a_{22}/a_{12}+1/Z_1+1/Z_3}}$	$Z_1+Z_3+g_m Z_1 Z_4$ $+\frac{(Z_1+Z_2+Z_3)(Z_4+Z_5)}{Z_2}=0\vert_{\substack{r_e=0\\ \beta=\infty}}$	$Z_1+Z_3+g_m Z_1 Z_4$ $+\frac{(Z_1+Z_2+Z_3)(Z_4+Z_5)}{Z_2}=0\vert_{\substack{r_s=0\\ r_{ds}=\infty}}$

The transmission matrix in this case can be shown to be

$$\begin{pmatrix} a_{11} & a_{12} \\ a_{21} & a_{22} \end{pmatrix} = \frac{1}{r_{ds}(1-g_m Z)+r_s} \times \begin{pmatrix} r_{ds}(1+g_m r_s)+Z & r_{ds}(1+g_m r_s)Z \\ 1+g_m r_{ds} & r_{ds}(1+g_m r_s) \end{pmatrix} \quad (24)$$

where $Z=1/sC_{gd}$. If we wish to consider the effect of this particular parasitic on any of the Colpitts oscillator topologies, we may directly substitute with the above matrix elements in Table 1 expressions. Further, and since transmission parameters are well-suited for networks in cascade, we may additionally incorporate the effects of C_{gs} and C_{ds} via matrix multiplication with (24) in the order of the cascade yielding

$$\begin{pmatrix} 1 & 0 \\ sC_{gs} & 1 \end{pmatrix} \begin{pmatrix} a_{11} & a_{12} \\ a_{21} & a_{22} \end{pmatrix} \begin{pmatrix} 1 & 0 \\ sC_{ds} & 1 \end{pmatrix}$$

Table 2 Comparison of the Colpitts oscillator circuits in Fig. 1

Circuit	Topology	Order	Ideal start-up condition	Oscillation frequency (ω_o)
Fig. 1*a*	common-A	2	$\frac{L/C_1}{r}=\frac{1}{g_m}$	$\sqrt{\frac{1}{LC_{eff}}-\left(\frac{r}{L}\right)^2}$
Fig. 1*b*	common-B	3	$\frac{L/(C_1+C_2)}{r}=\frac{1}{g_m}$	$1/\sqrt{LC_{eff}}$
Fig. 1*c*	common-A	2	$\frac{L/C_1}{R_E}=\frac{1}{g_m}\vert_{r=0}$	$\sqrt{\frac{L+rR_EC_1}{LC_{eff}(L-R_E^2C_1)}-\frac{r^2}{L^2-R_E^2C_1L}}$
Fig. 1*d*	common-A	2	$\frac{r}{1+(C_1/C_2)}=\frac{1}{g_m}$	$1/\sqrt{LC_{eff}}$
Fig. 1*e*	modified common-C	3	$\frac{R_C}{C_1/C_2}=\frac{1}{g_m}\vert_{r=0}$	$\sqrt{\frac{1}{LC_{eff}}+\frac{r}{L(R_E+R_C)C_2}}$

$$= \begin{pmatrix} a_{11} + sC_{ds}a_{12} & a_{12} \\ a_{21} + sC_{gs}(a_{11} + sC_{ds}a_{12}) + sC_{ds}a_{22} & a_{22} + sC_{gs}a_{12} \end{pmatrix} \quad (25)$$

For demonstration, let us consider for example the effect of a C_{gs} parasitic capacitor on a MOS-based common-A topology. Using (5), the MOS transistor transmission matrix with this parasitic included becomes

$$\begin{pmatrix} 1 & 0 \\ sC_{gs} & 1 \end{pmatrix} \cdot \begin{pmatrix} \frac{-1}{g_m r_{ds}} & -(r_s + 1g_m) \\ 0 & 0 \end{pmatrix} = -\begin{pmatrix} \frac{1}{g_m r_{ds}} & \left(r_s + \frac{1}{g_m}\right) \\ \frac{sC_{gs}}{g_m r_{ds}} & s\left(r_s + \frac{1}{g_m}\right)C_{gs} \end{pmatrix} \quad (26)$$

from which it is clear that both a_{11} and a_{12} are independent of C_{gs}. Noting that the common-A characteristic equation expression in Table 1 depends only on a_{11} and a_{12} implies that this oscillator is not affected by C_{gs}.

Alternatively, let us consider the effect of C_{ds} on the same oscillator. Using (5), the MOS transistor transmission matrix with this parasitic included becomes

$$\begin{pmatrix} \frac{-1}{g_m r_{ds}} & -\left(r_s + \frac{1}{g_m}\right) \\ 0 & 0 \end{pmatrix} \cdot \begin{pmatrix} 1 & 0 \\ sC_{ds} & 1 \end{pmatrix} = -\begin{pmatrix} \frac{1}{g_m r_{ds}} + s\left(r_s + \frac{1}{g_m}\right)C_{ds} & -\left(r_s + \frac{1}{g_m}\right) \\ 0 & 0 \end{pmatrix} \quad (27)$$

which shows that a_{11} is affected by C_{ds}. Substituting in the expression from Table 1 after setting $Z_1 = 1/sC_1$, $Z_2 = 1/sC_2$ and $Z_3 = sL + r$ yields

$$s^2 + \frac{C_1 r(C_2 + C_{ds}) - g_m LC_2}{LC_1(C_2 + C_{ds})}s + \frac{C_1 + C_2}{LC_1(C_2 + C_{ds})} = 0 \quad (28)$$

from which the oscillation start-up condition and the oscillation frequency are respectively

$$\frac{L/r}{C_1(1 + C_{ds}/C_2)} = \frac{1}{g_m} \text{ and } \omega_o = \frac{1}{\sqrt{L\{C_1(C_2 + C_{ds})/C_1 + C_2\}}} \quad (29)$$

More comprehensive transistor transmission matrices, which take into effect noise sources, can also be derived and used directly to evaluate the Colpitts oscillator performance.

5 Two-impedance two-port structures

In the previous section, we derived the characteristic equations for the three possible 'three-impedance' two-port structures and applied them particularly to the Colpitts oscillator. For completeness, the characteristic equations for the 'two-impedance' structures shown in Fig. 5, were derived and are shown in Table 3.

It can be seen from Table 3 that Fig. 5*a* cannot yield an oscillator if implemented using a BJT since Z_2 disappears from the characteristic equation. It can neither be implemented using a MOS transistor since the characteristic equation in this case reduces to $(1 - a_{11})Z_1 - a_{11}Z_2 - a_{12} = 0$, which cannot be satisfied with any positive $Z_{1,2}$ since a_{11} and a_{12} are both negative [recall (5)]. It can, however, be shown that with a transmission matrix of the form $a_{11} = 1/K$, $a_{12} = a_{21} = a_{22} = 0$, the characteristic equation $(K - 1)Z_1 - Z_2 = 0$ results and yields the classical Wien bridge oscillator for the choice of $Z_1 = R_1/(1 + R_1C_1s)$, $Z_2 = R_2 + 1/C_2s$ and $K > 0$ (non-inverting amplifier with gain K).

It can be similarly shown that the structure in Fig. 5*b* cannot oscillate for any positive Z_1 or Z_2 using the BJT or MOS transistors. However, for the choice of $a_{11} = k_1$, $a_{22} = k_2$ and $a_{12} = a_{21} = 0$, the characteristic equation $KZ_1 - Z_2 = 0$ can be obtained and can oscillate with the same $Z_{1,2}$ as the Wien bridge oscillator and also with $K > 0$. The start-up condition is $K = (R_2/R_1) + (C_1/C_2)$ and the oscillation frequency is $\omega_o = 1/\sqrt{R_1R_2C_1C_2}$. It is also possible to investigate other special transmission

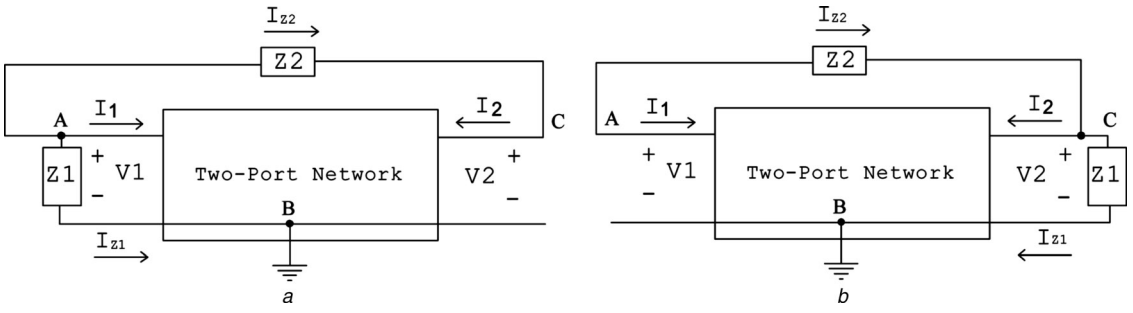

Figure 5 *Possible two-impedance two-port networks*

doi: 10.1049/iet-cds.2009.0062

Table 3 Summary of characteristic equations for the structures in Fig. 5

Figure	Characteristic equation	Special case
5*a*	$\frac{a_{12}+Z_2}{a_{22}-(1+Z_2/Z_1)}=\frac{a_{12}+a_{11}Z_2}{a_{21}Z_2+a_{22}-1}$	$(K-1)Z_1-Z_2=0$ if $(a)=\begin{pmatrix}\frac{1}{K} & 0\\ 0 & 0\end{pmatrix}$
5*b*	$\frac{a_{12}+Z_2}{a_{22}-1}=\frac{a_{11}Z_2+a_{12}(1+Z_2/Z_1)}{a_{21}Z_2+a_{22}(1+Z_2/Z_1)-1}$	$KZ_1-Z_2=0$ if $(a)=\begin{pmatrix}k_1 & 0\\ 0 & k_2\end{pmatrix}$ $K=(1+k_1k_2-k_1-k_2)/k_2$

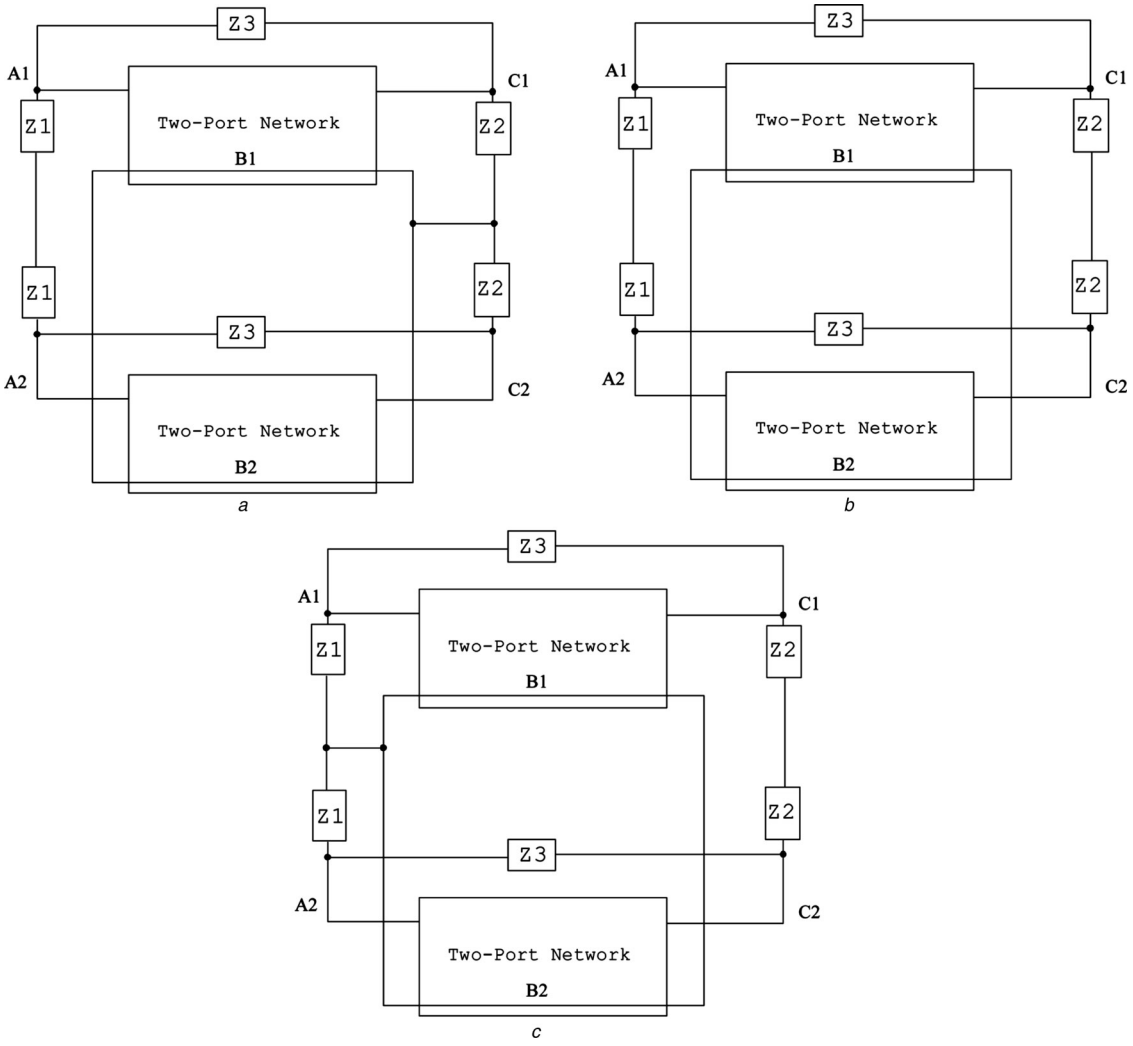

Q3 **Figure 6** *Three possible differential oscillator structures*

matrices, such as that of the gyrator (The gyrator transmission matrix is $\begin{pmatrix}a_{11} & a_{12}\\ a_{21} & a_{22}\end{pmatrix}=\begin{pmatrix}0 & r\\ 1/r & 0\end{pmatrix}$ where r is the gyration resistance.) in conjunction with other choices for Z_1 and Z_2 different from those in Table 3.

Q5

6 Conclusion

In this work, the general characteristic equations for a two-port network with three impedances and two impedances were derived. Application to the Colpitts oscillator

impedance setting implies three distinct classes of the oscillator as summarised in Table 1. The equations derived may be

1. Extended to any active device using its corresponding transmission matrix

2. Used no matter how sophisticated a transistor model becomes since all equations are functions of the transmission matrix elements

3. Used to explore unknown oscillator topologies via exhaustive testing of all possible impedance settings in association with a specific active device

Further, the use of two-port network structuring facilitates transforming single-ended topologies into differential ones. This is demonstrated in Fig. 6 which shows three possible differential topologies derived from the single-ended common-A, B and C structures, respectively.

7 References

[1] ALEXANDER C., SADIKU M.: 'Fundamentals of electric circuits' (McGraw-Hill International Edition, Singapore, 2000)

[2] BAYARD M.: 'Theorie des resaux de Kirchoff' (Ed. Rev. d'Optique, Paris, 1954)

[3] YODPRASIT U., ENZ C., GIMMEL P.: 'Common-mode oscillation in capacitive coupled differential Colpitts oscillators', *Electr. Lett.*, 2007, **43**, pp. 1127–1128

[4] JANG S., LEE S., CHIU C., CHUANG Y.: 'A 6 GHz, low power differential VCO', *Microw. Opt. Tech. Lett.*, 2007, **49**, pp. 76–79

[5] YAN S., ZHIGONG W., WEI L., LI Z.: 'Design and measurement of a 53 GHz balanced Colpitts oscillator', *Chin. J. Semicond.*, 2009, **30**, in press (DOI: 10.1088/1674–4926/30/1/015003)

[6] KENNEDY M.: 'Chaos in the Colpitts oscillator', *IEEE Trans. Circ. Syst.-I*, 1994, **41**, pp. 771–774

[7] MAGGIO G., DI BERNARDO M., KENNEDY M.: 'Nonsmooth bifurcations in a piecewise-linear model of the Colpitts oscillator', *IEEE Trans. Circ. Syst.-I*, 2000, **47**, pp. 1160–1177

[8] MAGGIO G., DE FEO O., KENNEDY M.: 'Nonlinear analysis of the Colpitts oscillator and applications to design', *IEEE Trans. Circ. Syst.-I*, 1999, **46**, pp. 1118–1130

[9] ELWAKIL A., KENNEDY M.: 'A family of Colpitts-like chaotic oscillators', *J. Franklin Inst.*, 1999, **336**, pp. 687–700

[10] RADWAN A., ELWAKIL A., SOLIMAN A.: 'Fractional-order sinusoidal oscillators: design procedure and practical examples', *IEEE Trans. Circ. Syst.-I*, 2008, **55**, pp. 2051–2063

[11] ELWAKIL A.: 'Explaining latchup in a classical Wien oscillator', *J. Analog Integ. Circ. Signal Process.*, 2006, **48**, pp. 239–245

[12] WALDHAUER F.: 'Feedback' (Wiley, NewYork, 1982)

[13] MAYARAM K.: 'Output voltage analysis for the MOS Colpitts oscillator', *IEEE Trans. Circ. Syst.-I*, 2000, **47**, pp. 260–263

[14] ANDREANI P., WANG X., VANDI L., FARD A.: 'A study of phase noise in Colpitts and LC tank CMOS oscillators', *IEEE J. Solid-State*, 2005, **40**, pp. 1107–1109

[15] FILANOVSKY I., VERHOEVEN C., REJA M.: 'Remarks on analysis, design and amplitude stability of MOS Colpitts oscillator', *IEEE Trans. Circ. Syst.-II*, 2007, **54**, pp. 800–804

[16] FARD A., ANDREANI P.: 'An analysis of $1/f^2$ phase noise in bipolar Colpitts oscillators (with a digression on bipolar differential-pair LC oscillators)', *IEEE J. Solid-State*, 2009, **42**, pp. 374–384

[17] WATANABE Y., KOMINE S., UCHIDA T.: 'Near carrier phase noise characteristics of narrow band Colpitts oscillators'. Proc. IEEE Ultrasoincs, Ferroelectrics and Frequency Control Conf., Montreal, Canada, 2004, pp. 457–461

[18] CHEN Y., MOUTHAAN K., OOI B.: 'Performance enhancement of Colpitts oscillators by parasitic cancellation', *IEEE Trans. Circ. Syst.-II*, 2008, **55**, pp. 1114–1118

doi: 10.1049/iet-cds.2009.0062

CDS57344

Author Queries

A.S. Elwakil

Q1 Please check if it is 'Electronic' or 'Electrical' and confirm the change of 'Emirates' to 'United Arab Emirates' ok, in the affiliation of the author.

Q2 Please provide the fullform of 'MOS' and 'BJT", 'NPN BJT '.

Q3 Please provide the sub-caption for Figs. 1, 5, 6.

Q4 Please provide a main caption for Fig. 2.

Q5 Footnote 1 has been moved to text as required by journal style. Please check and confirm that they have been located correctly within text.

Q6 Please provide page numbers for Ref. [5].

Dr Ahmed S Elwakil
Dept of electrical and computer engineering
P.O. Box 27272
Sharjah
United Arab Emirates

Reference: Item Number 0062G Ref. Id: CDS-2009-0062
On The Two-Port Network Classification of Colpitts Oscillators

IET– PROOFS

Please check the enclosed proofs carefully. The ultimate responsibility for the accuracy of the information contained within the paper lies with the author.

However, only essential corrections should be made at this stage and the proofs should not be seen as an opportunity to revise the paper.

Please return all corrections to this office by the date on the proof. Late corrections may not be included.